

Article

Applying a Simple Analytical Solution to Modelling Wind-Driven Coastal Upwelling of Two-Layered Fluid at the Head of Tokyo Bay, Japan

Zhongfan Zhu ^{1,*} , Xiaomei Bai ¹, Jie Dou ²  and Pengfei Hei ^{3,*}

¹ College of Water Sciences, Beijing Normal University, Beijing 100875, China; bxm@mail.bnu.edu.cn

² Center for Spatial Information Science, The University of Tokyo, Kashiwa 277-8568, Japan; douj888@gmail.com

³ College of Life and Environmental Science, Minzu University of China, Beijing 100081, China

* Correspondence: zhuzhongfan1985@bnu.edu.cn (Z.Z.); heipf06@mails.tsinghua.edu.cn (P.H.); Tel.: +86-10-5880-2739 (Z.Z.)

Received: 4 August 2017; Accepted: 26 September 2017; Published: 29 September 2017

Abstract: Blue tides at the head of Tokyo Bay are a hydro-environmental phenomenon where seawater appears to be milky blue because of the reflection of the sunlight off surface water containing large amounts of sulphur particles. Its appearance is due to the coastal upwelling of bottom oxygen-depleted water induced by northeasterly wind-driven circulation. Blue tides cause the death of many shellfish and other aquatic animals across the head of Tokyo Bay and consequently result in substantial economic losses to coastal fisheries. This paper examines the occurrence of wind-driven blue tides in Tokyo Bay, based on a simplified hydrodynamic model and observational analysis. The model assumed a two-layer structure with a wind-driven upper layer and an oxygen-depleted lower layer. In this study, we derived a simple analytical solution to determine a critical wind condition for which the lower layer outcrops at the surface if the wind forcing is sufficiently strong, resulting in the mixing of the two layers and giving rise to blue tide. The results of sensitivity analyses of the analytical solution to all incorporated factors were found to be in accordance with a qualitative understanding of the blue tide phenomenon. More importantly, comparisons of observational data with real cases of blue tide during 1978–2016 and without blue tide during 2003–2016 suggested that this analytical solution was mostly valid. This study would be helpful for gaining a better understanding of the hydro-dynamical mechanism of blue tide.

Keywords: coastal upwelling; blue tide; Tokyo Bay; analytical solution; sensitivity analysis

1. Introduction

Tokyo Bay is a typical semi-enclosed embayment subject to eutrophication [1–3]. The input of nutrient loads, with available sunlight at the surface and suitable temperatures in spring or summer, promote the excessive growth and decay of phytoplankton [1,2,4]. When the phytoplankton die and fall into the lower water due to gravity, some are decomposed by bacteria at the bottom, and the nutrients contained in the organic matter are converted into inorganic forms [2,5]. During this process, a large concentration of dissolved oxygen at the bottom is consumed, and the bottom water consequently becomes oxygen-depleted and even anoxic. On the other hand, along the seasonal temperature stratifications, fresh water inflows around the bay and intermittent precipitation result in a high-temperature, low-salinity upper water layer and a low-temperature, high-salinity lower water layer [6–9]. As a result, a stable density stratification forms in which the lighter upper water overlies the heavier lower water, hindering the vertical circulation that brings dissolved oxygen from the surface to the bottom and thus enhances the oxygen-depleted state of the lower water [5,8]. Under anaerobic

conditions, sulphate contained in the bottom water will be reduced to hydrogen sulphide and other sulphide forms by redox cells of sulphate. As northeasterly winds begin to blow on the surface, the upper layer water will follow the wind in the downwind direction. The lower water will flow in the opposite direction to compensate, and with the aid of bottom topography, the water can up well to the surface at the head of the bay (i.e., the northeast shore) [5–8,10–13]. Accompanying this upwelling process, a large amount of hydrogen sulphide and sulphide present in the lower water is oxidized to colloidal sulphur substances when it meets the oxygen in the atmosphere near the surface. When sunlight reflects off the surface water in which these sulphur particles are suspended, the colour of the seawater rapidly turns a milky blue or blue-green, a phenomenon that has been termed “blue tide” [5,7,14]. Most blue tides occur at the head of Tokyo Bay, from the northeast shore to the southeast shore, ranging from off Urayasu to off Ichihara [3,5,11,13]. The upwelling of oxygen-depleted bottom water causes widespread mortality in fish and shellfish living in the upper water layer and consequently leads to substantial economic losses to coastal fisheries [2,8,13].

Blue tide has been investigated by many researchers, especially Japanese researchers. Kakino et al. [6] studied the relationship between blue tide and wind-driven current and found that there is a good correlation between one-day averaged off-shore wind speed and one-day averaged movement speed of the bottom sulphide-containing water. Kataoka et al. [7] analysed the data from a blue tide that occurred from 11 August to 14 September in 1987 and noted that there were two important processes that finally led to the occurrence of a blue tide: the formation of oxygen depleted water at the bottom of the bay (biological, chemical process) and upwelling of this oxygen depleted water caused by the continual presence of the northeasterly wind (physical process). Matsuyama et al. [15] conducted a numerical experiment to clarify the mechanism of the generation and propagation of blue tide in Tokyo Bay during the period from summer to early fall. Moreover, Nakatsuji et al. [16] carried out a simple two-dimensional visualization experiment to demonstrate the upwelling and mixing phenomena of a stratified two-layer fluid system under different wind conditions and stratification degrees. More systematic research in this respect can be found in Yoon et al. [17–19]. An interdisciplinary field survey of blue tide was conducted by Otsubo et al. [5] on 5 September and 8 September 1988 in Tokyo Bay, and two hydraulic mechanisms of the occurrence of blue tide were proposed. Some researchers performed numerical simulations to investigate the movement of the bottom oxygen-depleted water that finally leads to the occurrence of blue tide [10–13,20–22]. For the occurrence of a blue tide that only occurred off Yokohama (the western side of the bay) in 2004, Koibuchi and Isobe [23] analysed the reason based on field observation data and numerical simulation and noted that the southerly wind and certain conditions of the density stratification played a decisive role in this real case. In addition, Sasaki et al. [11,24], Sasaki [4], and Ichioka et al. [25] investigated the amount of sulphide contained in the dredged trenches and/or navigation channels at the head of Tokyo Bay and clarified their contributions to the understanding of the occurrence of blue tide by using numerical experiments. Recently, Higa et al. [3] estimated the spatial distribution of blue tide at the head of Tokyo Bay based on the observational results of the optical properties of satellite images and numerical simulation with three-dimensional hydrodynamic and ecological models.

Moreover, in order to simply estimate the northeasterly wind conditions for the occurrence of blue tide in Tokyo Bay, Zhu [8] derived an analytical solution to estimate the critical wind conditions for the occurrence of blue tide on the southeast shore of the bay, using a two-layered fluid model consisting of an upper water layer and a bottom oxygen-depleted water layer. For the occurrence of blue tide on the northeast shore at the head of Tokyo Bay, Zhu and Yu [9] also presented a new analytical solution to determine the speed of the northeasterly wind that finally leads to the occurrence of blue tide. However, the proposed analytical solution was based on a small-amplitude assumption that the magnitudes of the surface and the density interface between the two-layer fluids are small compared with the thicknesses of the upper and bottom water layers so that they could be negligible, which greatly simplifies the governing equations to facilitate the derivations of the analytical solutions. This assumption is obviously incompatible with the fact that an outcrop of the bottom oxygen-depleted

water leads to the occurrence of blue tide. On the other hand, although the proposed analytical solution showed its validity, its comparison with real cases without blue tide was not performed in the study of Zhu and Yu [9], which seemingly implies that the wind conditions presented by the analytical solution are not the critical conditions for the occurrence of blue tide at the head of Tokyo Bay. In this study, we relaxed the small-amplitude assumption and derived a simple analytical solution to determine the wind conditions for the occurrence of blue tide on the northeast shore at the head of the bay in the context of a two-layered fluid. Further, although the analytical solution is simple and based on some assumptions and simplifications, comparison of both real cases with blue tides during 1978–2016 and real cases without blue tides during 2003–2016 showed that it is mostly valid.

There seem to be few mesh-based numerical model studies to specifically investigate the critical wind conditions for the occurrence of blue tide at the head of Tokyo Bay. Compared to the numerical modelling approach and laboratory experimental approach, the analytical approach adopted in this study is able to roughly estimate the conditions under which blue tide occurs at the head of the bay with lesser computational cost, and it also helps us to gain a qualitative understanding of the factors that influence the occurrence of blue tide and what these effects are, based on some simplifications and assumptions. On the other hand, a numerical simulation with large computational cost seems to be incapable of achieving these aims.

This study is arranged as follows. Section 2 introduces a simple hydrodynamic explanation for the occurrence of blue tide at the head of Tokyo Bay and derives a simple analytical solution to determine a critical wind condition under which the lower layer outcrops, resulting in the mixing of the two-layered fluid and giving rise to a blue tide. Sensitivity analyses of the analytical solution to all the incorporated factors are also performed in this section. Section 3 presents the comparison of the proposed analytical solution with real cases of blue tides during 1978–2016 and without blue tides during 2003–2016. Finally, a simple discussion and concluding remarks are given in Section 4.

2. Simple Explanation for Blue Tide Occurrence and Derivation of the Analytical Solution

As shown in Figure 1, Tokyo Bay is located in the central part of the main island (Honshu) of Japan. The bay, bordered by the vast Kanto region to the north, the Boso peninsula to the east and the Miura peninsula to the west, is a semi-enclosed estuarine embayment that faces the Pacific Ocean through a narrow waterway (Kannonzaki to Futsumisaki waterway). The length of Tokyo Bay's coastline is almost 890 km, and its area covers approximately 922 km² [26]. The bay stretches approximately 60 km along its major length and 20 km along its minor length, and the average water depth is 15 m, with the western side being deeper than the eastern side [1,2,26,27].

The analytical solution was based on the following two large simplifications:

- (1) Although the actual coastline of Tokyo Bay is irregular, the chosen domain was considered to be a rectangular flat domain 50 km in length, 20 km in width and with an average water depth of 15 m, as indicated by three solid red lines and a dashed red line showing the imaginary southwest shore in Figure 1. The remaining 10 km is the outer bay, which does not have not much exchange with the inner bay, as shown by many studies [15,22,26,28]. Figure 2a schematically shows the dimensions of the chosen research domain, where L is the length, and in the right-handed Cartesian coordinate system, the x axis follows the northeasterly wind, the y axis is perpendicular to the length direction, and the z axis is positive in the upward direction relative to the quiescent surface water level;
- (2) A simple two-layered fluid model consisting of an upper wind-driven water layer and a bottom oxygen-depleted water layer was adopted to represent the actual stratified flow in Tokyo Bay. Similar studies have been carried out by Otsubo et al. [5], Nakatsuji et al. [16] and Yoon et al. [17–19]. Figure 2b schematically shows this conceptual two-layered fluid model.

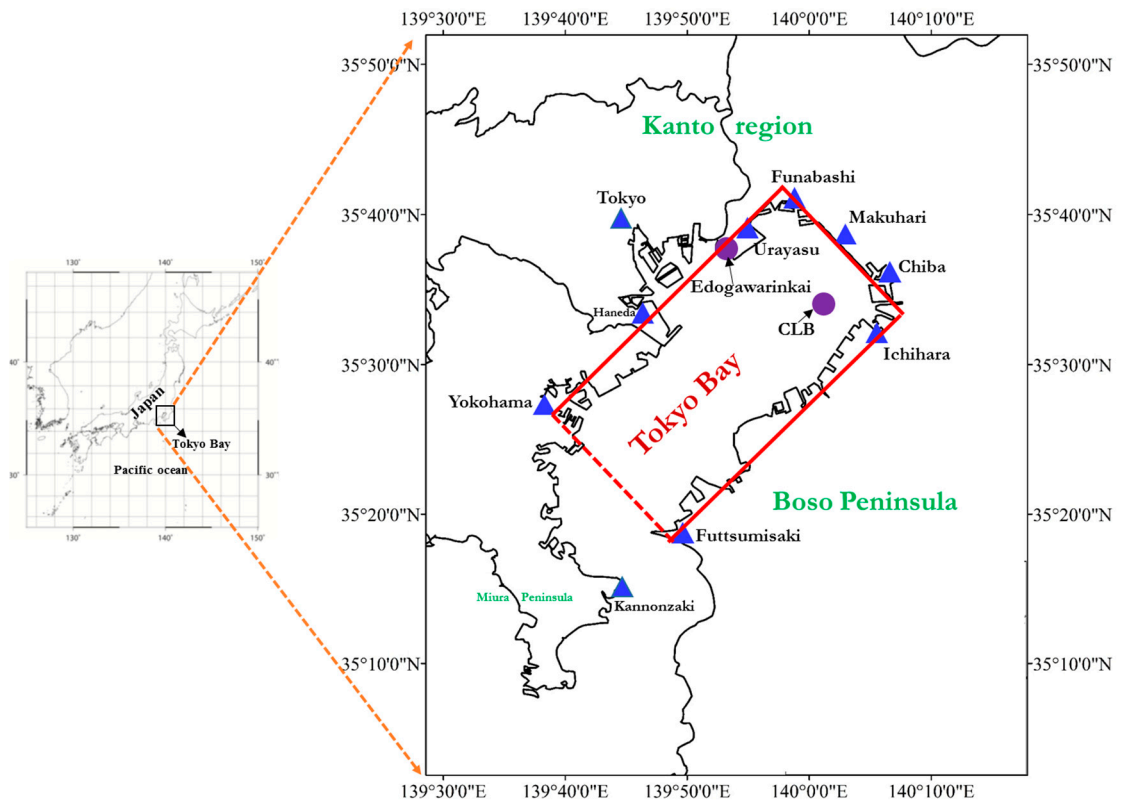
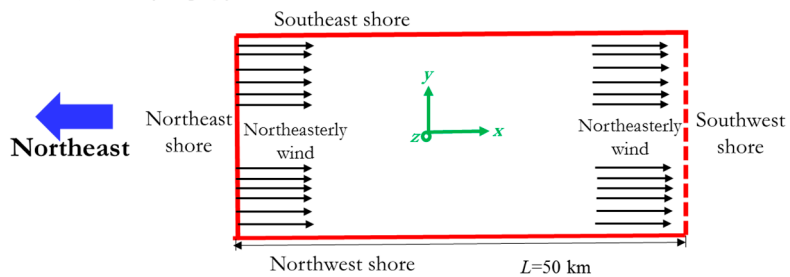


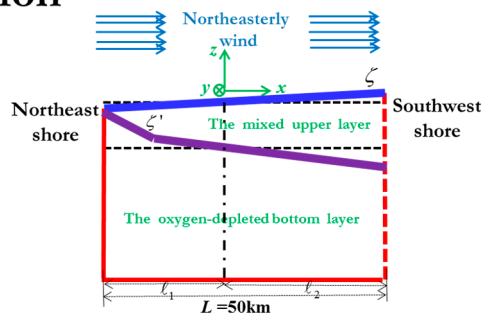
Figure 1. Map of the geographic location of Tokyo Bay and the chosen research area for the study of coastal upwelling.

Plan view



(a)

Cross section



(b)

Figure 2. (a) Dimensions of the chosen research area and (b) a schematic diagram of coastal upwelling on the northeast shore induced by northeasterly wind-driven circulation in the context of a two-layered fluid model.

We attempted to present a conceptual interpretation for the occurrence of blue tide at the head of the bay from a hydrodynamic viewpoint. Considering a northeasterly wind across the entire bay, at short timescales, the influence of the Coriolis force could be negligible so that the wind-driven motion of the two-layered fluid can be considered to be in the $x - z$ longitudinal section. As Figure 2b shows, the water layer beneath the surface will follow the northeasterly wind in the downwind direction, leading to the tilt of the surface with up on the southwest shore and down on the northeast shore. The rest of the water layer between it and the density interface will flow in the upwind direction. The pressure gradient due to the surface tilt will induce the bottom water to move towards the northeast shore, which induces the density interface to rise on the northeast shore and drop on the southwest shore. The direction of the tilt of the density interface is opposite to that of the surface. If the wind forcing is sufficiently strong, the density interface will intersect the surface. At this time, a large amount of hydrogen sulphide contained in the bottom water layer will meet oxygen at the surface, and as a result, the blue tide phenomenon can occur on the northeast shore of the bay. At long timescales of the northeasterly blowing wind, the two-layered fluid will be deflected to the right of the wind direction due to the Coriolis force. This simple hydrodynamic explanation to the blue tide occurrence was found to be consistent with some previous studies [5–7,9,12,15]. Although it seems difficult to determine the specific time at which the Coriolis force starts to play a role, this time scale could be simply estimated as two days in this study based on the numerical experiments of Matsuyama et al. [15] and Ueno et al. [28] concerning coastal upwelling in Tokyo Bay. Considering that this study focused on blue tides on the northeast shore at the head of the bay, the influence of the Coriolis force could be regarded as negligible when the northeasterly wind did not exceed two days in this preliminary study, greatly facilitating the derivations of the analytical solution. Thus, after further neglecting the non-linear terms that were considered to be negligible by Csanady [29] for large stratified lakes or estuarine bays, rewritten as the momentum and continuity equations for the upper and lower layers, they are, respectively:

The upper layer:

$$\frac{\partial u}{\partial t} = -g \frac{\partial \zeta}{\partial x} + \frac{\tau_s}{\rho(h + \zeta - \zeta')} - \frac{\tau_I}{\rho(h + \zeta - \zeta')}, \quad (1)$$

$$\frac{\partial [u(h + \zeta - \zeta')]}{\partial x} = -\frac{\partial (\zeta - \zeta')}{\partial t}; \quad (2)$$

The bottom layer:

$$\frac{\partial u'}{\partial t} = -g \frac{\rho}{\rho'} \frac{\partial \zeta}{\partial x} - g \varepsilon \frac{\partial \zeta'}{\partial x} + \frac{\tau_I - \tau_B}{\rho'(h' + \zeta')}, \quad (3)$$

$$\frac{\partial [u'(h' + \zeta')]}{\partial x} = -\frac{\partial \zeta'}{\partial t}; \quad (4)$$

where u and u' are the vertically averaged horizontal velocities in the x direction for the upper layer and the lower one, respectively, ζ and ζ' are the displacements of the surface and density interface, respectively, τ_s is the surface-wind stress in the x direction, τ_I and τ_B are the interfacial friction and bottom friction for the two-layered fluid in the x direction, respectively, h and h' are the thicknesses of the upper and lower layers, respectively, ρ and ρ' are the densities of the upper and lower layers, respectively, with the density contrast, ε , between such two layers being ($\varepsilon = (\rho' - \rho)/\rho'$), g is the gravitational acceleration, and t is the time. As Figure 2b illustrates, we conveniently chose the origin point of the right-handed coordinate system to be the point at which both the surface displacement ζ and the interfacial displacement ζ' are zero, and ℓ_1 and ℓ_2 are the distances between the northeast shore and the origin and between the southwest shore and the origin, respectively. Moreover, in order to derive the analytical solution, we considered a specific steady state in which the displacement of the interface intersects the surface displacement on the northeast shore. At this point, there is a clockwise circulation in the upper mixed water layer and an anti-clockwise circulation in the bottom water layer, so that $u = 0$ and $u' = 0$. Further, if we assume that the interfacial friction can be expressed

as proportional to the velocity difference between the upper and lower layers and that the bottom friction can be expressed as proportional to the velocity of the bottom layer, it can be readily found that $\tau_I = \tau_B = 0$ in this study. Substituting such conditions into Equations (1)–(4) and considering the critical conditions for the occurrence of blue tide, i.e., $\zeta'(-\ell_1) + |\zeta(-\ell_1)| = h$, can give rise to

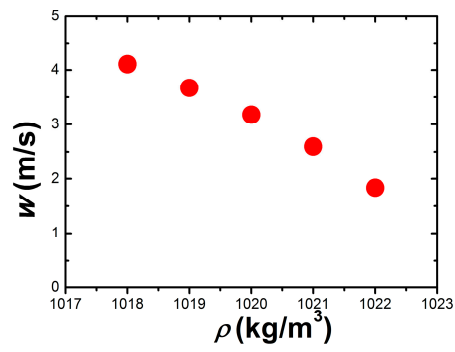
$$\zeta(x) = \frac{\varepsilon}{\varepsilon - 1} \zeta'(x), \text{ and } \zeta'(x) = h(1 - \varepsilon) - \sqrt{h^2(1 - \varepsilon)^2 + \frac{2\tau_s(1 - \varepsilon)^2}{\rho g \varepsilon}} x, \quad (5)$$

$$\frac{\ell_2}{\ell_1} = \frac{5}{4}, \text{ and } \frac{\tau_s}{\rho} = \frac{9}{8} \frac{g \varepsilon h^2}{L}; \quad (6)$$

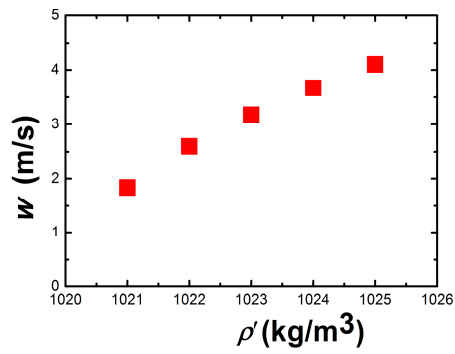
Note that the displacements of the surface and density interface, $\zeta(x)$, $\zeta'(x)$, are not linear functions of x , and further, it can be observed from Equation (5) that increasing wind stress τ_s/ρ gives rise to large values for $\zeta'(-\ell_1)$ and $|\zeta(-\ell_1)|$ here ($\zeta'(-\ell_1) + |\zeta(-\ell_1)| > h$). Thus, Equation (6) could represent the minimum wind stress for the occurrence of blue tides on the northeast shore of the research area. It should also be noted that there are some simplifications and assumptions involved in the derivation of the analytical solution, but it gives a simple relation for characterizing the dependence of wind conditions on the stratification properties and geometrical properties of the two-layered fluid. Furthermore, this proposed analytical solution shows its validity by comparison with real cases with and without blue tides as presented in the following section. Relaxing such simplifications and assumptions in the derivation process of the analytical solution should be worthy of further investigation in future research.

In general, surface-wind stress can be expressed as a quadratic function of wind speed as follows [14,15,26]: $\tau_s = \rho_a \gamma_a^2 w^2$, where ρ_a is air density (1.23 kg/m³ here), γ_a^2 is the surface-drag coefficient (here it can be taken as $\gamma_a^2 = 1.30 \times 10^{-3}$, as adopted by Matsuyama et al. [15], Suzuki and Matsuyama [26] and Takahashi et al. [14]), and w is the average wind speed measured 10 m above the still surface. Substituting this relation into Equation (6) could lead to the minimum wind speed for the blue tide occurrence on the northeast shore of the bay expressed as $w = 1.06h\sqrt{\rho g \varepsilon / \rho_a \gamma_a^2 L}$.

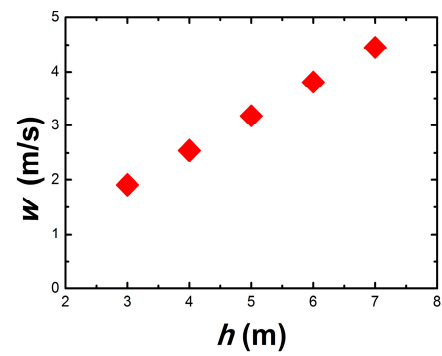
A simple graphic analysis is employed to explore the sensitivities of the analytical solution to the incorporated five parameters, i.e., the density of the upper layer ρ , the density of the bottom layer ρ' , the thickness of the upper layer h , the length of the research area L , and the surface-drag coefficient γ_a^2 , as shown in Figure 3. The typical parameter values for ρ , ρ' , h , L and γ_a^2 were $\rho = 1020$ kg/m³, $\rho' = 1023$ kg/m³, $h = 5$ m, $L = 50$ km, and $\gamma_a^2 = 1.3 \times 10^{-3}$ as shown in observational datasets of the stratification condition in Tokyo Bay in the next section. In the sensitivity analyses, all of the parameter values were kept constant as listed above, except for those mentioned.



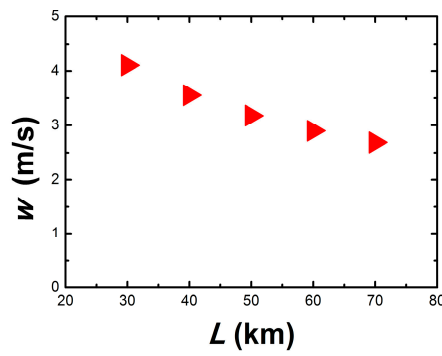
(a)



(b)



(c)



(d)

Figure 3. Cont.

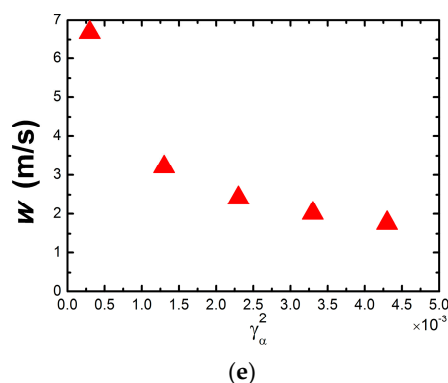


Figure 3. Sensitivity of the analytical solution to four incorporated parameters: (a) the density of the upper, well-mixed water layer; (b) the density of the bottom water layer; (c) the thickness of the upper, well-mixed water layer; (d) the length of the research area and (e) the surface-drag coefficient.

In the two-layered fluid system, either decreasing the density of the upper, well-mixed water layer (as presented in Figure 3a) or increasing the density of the bottom water layer (as presented in Figure 3b) means increasing the relative gravity of the bottom oxygen-depleted water layer against the surface wind effect, which makes coastal upwelling more difficult. This point agrees with the findings of a numerical experiment by Matsuyama et al. [15] on coastal upwelling in Tokyo Bay, which clearly showed that coastal upwelling is likely to occur in early autumn because the density stratification between the upper and bottom water layers in Tokyo Bay becomes weaker during that period. This point is also in accordance with the observational results of laboratory experiments of Yoon et al. [17–19] concerning wind-driven stratified flow in enclosed or open water bodies, which clearly indicated that the velocity of coastal upwelling is higher and the time needed for the density interface to reach the surface becomes shorter for the experimental cases with a small density contrast. Increasing the thickness of the upper water layer means lengthening the spatial distance of coastal upwelling on the northeast shore, which causes coastal upwelling to be more unlikely, as presented in Figure 3c. It is obvious from Figure 3d that coastal upwelling becomes easier as the length of the research area increases. A simple interpretation from a geometrical perspective is as follows. For a long research area, the imposed surface wind stress induces a large tilt of the surface, which leads to a large pressure gradient between the southwest shore and the northeast shore. This pressure gradient causes a large tilt of the density interface, which makes coastal upwelling more likely on the northeast shore. It can be found from Figure 3e that a large surface-drag coefficient means a strong surface wind stress, making coastal upwelling become easier on the northeast shore. These analyses were found to be consistent with a qualitative understanding of the wind-driven coastal upwelling.

3. Comparison with Observational Data

3.1. Handling of the Observational Datasets

We have collected complete observational datasets concerning the occurrence of wind-driven blue tides at the head of Tokyo Bay during 1978–2016. Datasets for 2001–2016 were provided as anoxic water reports from the Fisheries Research Center of Chiba Prefectural Government, Japan, and they can be downloaded from the Chiba prefecture homepage: <http://www.pref.chiba.lg.jp/lab-suisan/suisan/suikaisokuhou/index.html>; Early datasets during 1988–2000 are extracted from annual reports of the Chiba prefectural laboratory of water pollution, and more information can be found at the website: <http://www.pref.chiba.lg.jp/lab-suisan/index.html>; Earlier data during 1978–1987 could be found in the paper by Nakatsuji et al. [16].

Concerning the wind datasets, we simply adopted real-time sets measured at the Edogawarinkai station to represent the entire wind condition across the head of Tokyo Bay (as indicated in Figure 1)

considering the geographic distribution of measurement stations for wind conditions provided by the Japanese Meteorological Agency (JMA) in Tokyo Bay. These datasets during 1978–2016 can be downloaded from the official website of the JMA: <http://www.data.jma.go.jp/obd/stats>. Furthermore, we used the hourly wind datasets (including wind speed and wind direction) that are the most accurate at present to calculate the average wind speed before each occurrence of blue tide on the northeast shore of the bay.

The density contrast and thicknesses of the upper, well-mixed water layer presented in the analytical solution needs to be estimated for all real cases of blue tides. To calculate two such parameters, we simply used the real-time datasets of water quality monitoring measured by the Chiba Light Beacon (CLB) provided by the Hydrographic and Oceanographic Department (HOD) of the Japanese Coast Guard (JCG) (the geographic location of the CLB was also indicated in Figure 1) to represent the entire stratification condition across the head of Tokyo Bay. These datasets include water temperature, salinity, dissolved oxygen, chlorophyll a and turbidity, and they can be extracted from the official website: <http://www4.kaiho.mlit.go.jp/kaihoweb>. Once the temperature and salinity values of the surface layer water and bottom layers water are known, the densities of the upper, well-mixed water layer and the bottom, oxygen-depleted water layer can be calculated using the formula presented in McCutcheon et al. [30], used by many researchers [31–36]. The thickness of the upper, well-mixed water layer can be estimated from the vertical distribution of dissolved oxygen together with water temperature and salinity provided by the CLB. Nevertheless, the earliest observational dataset provided by the CLB started from 2003. To this end, for those real cases of blue tides during 1978–2002 that lack real-time observational data, we simply adopted the algebraically averaged density values of the upper and bottom water layers for every month from 2003 to 2016 to be representative of real cases observed from 1978 to 2002 by mainly considering the seasonal variation of the stratification in Tokyo Bay. Table 1 presents monthly mean temperature values, salinity values, calculated monthly mean density values and algebraically averaged density values of the upper, well-mixed layer and the bottom, oxygen-depleted layer during 2003–2016. Table 2 lists monthly mean values and algebraically averaged values of the thickness of the upper, well-mixed water layer during 2003–2016 based on real-time data taken at the CLB. Finally, it should be noted that this study did not use the spatially averaged wind data and stratification data in the bay, considering a lack of long-term real-time data taken at different locations except the CLB.

3.2. Comparison with Real Cases of Blue Tides on the Northeast Shore

Table 3 presents information regarding real cases of blue tides observed on the northeast shore of Tokyo Bay from 2003 to 2016. The first column shows the occurrence dates and areas of the blue tides. The measured average wind speed, w_{m1} , of the northeasterly wind before the occurrences of the blue tides is presented in the second column using measurement data from the Edogawarinkai station provided by the Japanese Meteorological Agency. Stratification conditions for the water body at the head of Tokyo Bay, including the temperature, salinity and density values of the upper, well-mixed and bottom, oxygen-depleted water layers and the thicknesses of the upper, well-mixed water layer are shown in the third column using measurement data from the CLB. Using these values, the analytical solution for each real case, i.e., the modelled wind speed, w_{m2} , could be calculated as presented in the last column. The results regarding whether the real cases satisfy the calculated analytical solution are presented in Figure 4, which indicates that eight of the nine real cases of blue tides on the northeast shore of Tokyo Bay agreed well with the proposed analytical solution.

Table 1. Monthly mean temperature values, salinity values, calculated monthly mean density values and algebraically averaged density values of the upper, well-mixed layer and the bottom, oxygen-depleted layer during 2003–2016.

Month	Year	Surface Temperature (°C)	Surface Salinity (psu)	The Upper Layer Density (kg/m ³)	Bottom Temperature (°C)	Bottom Salinity (psu)	The Lower Layer Density (kg/m ³)	Average Density Value of the Upper Layer (kg/m ³)	Average Density Value of the Bottom Layer (kg/m ³)
May	2003	19.00	29.80	1021.08	16.80	32.20	1023.44	1021.12	1023.06
	2004	18.00	30.20	1021.63	16.80	31.80	1023.13		
	2005	18.00	31.00	1022.24	16.80	32.60	1023.75		
	2006	18.00	30.20	1021.63	16.80	31.80	1023.13		
	2007	18.60	30.20	1021.48	18.00	31.40	1022.55		
	2008	16.80	31.00	1022.52	15.00	32.20	1023.84		
	2009	19.20	29.80	1021.03	16.80	31.40	1022.83		
	2010	18.00	29.00	1020.71	15.60	31.00	1022.79		
	2012	19.20	27.80	1019.51	16.80	31.00	1022.52		
	2014	20.40	29.40	1020.42	18.00	31.80	1022.85		
2015	20.40	29.00	1020.12	18.00	31.80	1022.85			
June	2003	22.80	29.00	1019.47	20.40	31.80	1022.25	1019.20	1022.75
	2004	22.80	27.80	1018.57	20.40	31.00	1021.64		
	2005	21.60	29.80	1020.41	18.00	32.60	1023.46		
	2006	20.40	29.00	1020.12	16.80	33.00	1024.05		
	2007	22.80	29.00	1019.47	19.20	31.80	1022.56		
	2008	21.60	27.00	1018.29	19.20	31.80	1022.56		
	2009	21.60	27.00	1018.29	18.00	31.40	1022.55		
	2010	21.60	28.00	1019.04	19.20	31.00	1021.95		
	2012	21.60	29.00	1019.80	19.00	31.80	1022.61		
	2014	21.80	27.80	1018.84	19.20	32.20	1022.86		
2015	21.60	27.80	1018.89	18.00	33.00	1023.77			
July	2003	22.80	29.00	1019.47	19.60	32.60	1023.06	1017.67	1021.96
	2004	26.40	28.20	1017.82	22.80	31.00	1020.99		
	2005	24.00	27.00	1017.63	20.40	32.20	1022.55		
	2006	24.00	28.20	1018.53	19.20	32.20	1022.86		
	2007	24.00	29.00	1019.14	20.40	32.60	1022.86		
	2008	26.40	25.00	1015.42	19.20	31.40	1022.25		
	2009	25.20	27.00	1017.28	21.60	30.20	1020.71		
	2010	26.40	27.00	1016.92	21.60	31.00	1021.32		
	2012	25.20	27.80	1017.88	20.40	31.00	1021.64		
	2014	26.40	26.60	1016.62	20.40	31.80	1022.25		
2015	24.00	27.00	1017.63	20.40	30.20	1021.03			

Table 1. Cont.

Month	Year	Surface Temperature (°C)	Surface Salinity (psu)	The Upper Layer Density (kg/m ³)	Bottom Temperature (°C)	Bottom Salinity (psu)	The Lower Layer Density (kg/m ³)	Average Density Value of the Upper Layer (kg/m ³)	Average Density Value of the Bottom Layer (kg/m ³)
August	2003	26.40	27.00	1016.92	22.80	30.60	1020.69	1016.91	1020.91
	2004	26.40	29.00	1018.42	25.20	31.00	1020.29		
	2005	27.60	25.00	1015.05	21.60	31.80	1021.93		
	2006	26.40	27.00	1016.92	19.20	31.80	1022.56		
	2007	28.20	27.00	1016.36	24.00	31.00	1020.65		
	2008	26.40	27.00	1016.92	24.00	31.00	1020.65		
	2009	26.40	27.80	1017.52	21.60	31.40	1021.62		
	2010	28.80	27.00	1016.16	25.20	31.00	1020.29		
	2012	27.80	27.80	1017.08	25.00	31.00	1020.35		
	2014	26.40	27.00	1016.92	24.00	29.80	1019.74		
2015	27.60	28.60	1017.75	22.80	31.40	1021.29			
September	2003	25.80	29.00	1018.60	22.80	31.00	1020.99	1018.93	1021.53
	2004	25.20	30.20	1019.69	24.00	31.40	1020.95		
	2005	25.20	27.00	1017.28	21.60	31.00	1021.32		
	2006	24.00	29.00	1019.14	21.60	32.20	1022.23		
	2007	25.20	29.00	1018.78	22.80	31.00	1020.99		
	2008	25.20	29.00	1018.78	22.80	32.60	1022.20		
	2009	22.80	31.00	1020.99	21.60	32.60	1022.53		
	2010	27.60	29.00	1018.05	24.00	32.20	1021.55		
	2012	27.60	29.00	1018.05	25.20	31.40	1020.59		
	2014	22.80	29.80	1020.08	21.60	32.60	1022.53		
2015	24.00	28.60	1018.83	22.80	31.00	1020.99			
October	2003	20.40	31.00	1021.64	19.80	32.20	1022.71	1020.92	1022.30
	2004	21.60	29.00	1019.80	21.60	32.20	1022.23		
	2005	21.60	31.00	1021.32	21.60	32.20	1022.23		
	2006	21.00	29.80	1020.57	21.00	32.20	1022.39		
	2007	21.60	29.00	1019.80	21.60	32.20	1022.23		
	2008	21.60	30.20	1020.71	21.60	32.60	1022.53		
	2009	21.60	31.00	1021.32	21.60	32.20	1022.23		
	2010	21.60	31.00	1021.32	21.60	33.00	1022.84		
	2012	20.40	31.40	1021.94	20.40	32.20	1022.55		
	2014	21.60	29.80	1020.41	21.60	32.60	1022.53		
2015	20.40	30.60	1021.33	20.40	31.80	1022.25			

Table 1. Cont.

Month	Year	Surface Temperature (°C)	Surface Salinity (psu)	The Upper Layer Density (kg/m ³)	Bottom Temperature (°C)	Bottom Salinity (psu)	The Lower Layer Density (kg/m ³)	Average Density Value of the Upper Layer (kg/m ³)	Average Density Value of the Bottom Layer (kg/m ³)
November	2003	18.00	31.00	1022.24	18.00	32.60	1023.46		
	2004	19.20	29.00	1020.42	19.20	31.80	1022.56		
	2005	18.00	31.00	1022.24	19.20	32.60	1023.17		
	2006	18.00	31.00	1022.24	18.00	32.20	1023.16		
	2007	18.00	31.00	1022.24	18.00	32.60	1023.46		
	2008	19.20	31.40	1022.25	19.20	32.20	1022.86	1021.94	1023.10
	2009	19.20	30.60	1021.64	19.20	31.80	1022.56		
	2010	18.00	29.80	1021.32	18.00	31.00	1022.24		
	2012	16.80	30.60	1022.21	15.60	31.80	1023.40		
	2014	18.00	31.40	1022.55	16.80	32.60	1023.75		
	2015	20.20	31.40	1021.99	18.00	32.60	1023.46		

Note: Real-time data for the stratification conditions in 2011, 2013 and 2016 measured at the CLB are lacking (<http://www4.kaiho.mlit.go.jp/kaihoweb>).

Table 2. Monthly mean values and algebraically averaged values of the thickness of the upper, well-mixed water layer during 2003–2016 based on real-time data taken at the CLB.

Month	Year	The Thickness of the Upper Layer (m)	Average Thickness Value of the Upper Layer (m)	Month	Year	The Thickness of the Upper Layer (m)	Average Thickness Value of the Upper Layer (m)
May	2003	4.00	5.00	September	2003	3.00	3.41
	2004	5.00			2004	5.00	
	2005	5.00			2005	3.00	
	2006	5.00			2006	3.00	
	2007	5.00			2007	3.00	
	2008	5.00			2008	3.00	
	2009	5.00			2009	2.00	
	2010	5.00			2010	3.00	
	2012	5.00			2012	3.00	
	2014	6.00			2014	5.00	
2015	5.00	2015	4.50				
June	2003	5.00	4.50	October	2003	4.00	3.95
	2004	4.50			2004	4.00	
	2005	5.00			2005	5.00	
	2006	3.00			2006	3.00	
	2007	5.50			2007	3.00	
	2008	4.00			2008	3.00	
	2009	5.00			2009	4.00	
	2010	5.00			2010	3.00	
	2012	4.00			2012	5.00	
	2014	4.00			2014	4.50	
2015	4.50	2015	5.00				
July	2003	3.00	4.09	November	2003	5.00	5.05
	2004	4.00			2004	4.00	
	2005	4.00			2005	5.00	
	2006	3.00			2006	5.00	
	2007	3.00			2007	5.00	
	2008	4.50			2008	5.00	
	2009	5.00			2009	5.00	
	2010	5.50			2010	5.00	
	2012	5.00			2012	5.50	
	2014	4.00			2014	5.50	
2015	4.00	2015	5.50				
August	2003	4.00	4.05				
	2004	5.00					
	2005	3.50					
	2006	3.00					
	2007	5.00					
	2008	4.00					
	2009	3.00					
	2010	5.00					
	2012	4.00					
	2014	4.00					
2015	4.00						

Note: Real-time data for the stratification conditions in 2011, 2013 and 2016 measured at the CLB are lacking (<http://www4.kaiho.mlit.go.jp/kaihoweb>).

Table 3. Information regarding real cases of blue tides observed on the northeast shore of Tokyo Bay during 2003–2016.

Blue Tide on the Northeast Shore of Tokyo Bay		Northeasterly Wind		Stratification Condition				The Analytical Solution	
Occurrence Date	Occurrence Area	Average Wind Speed (m/s)	Surface Temperature//Surface Salinity (°C)//(psu)	Bottom Temperature//Bottom Salinity (°C)//(psu)	The Upper Layer Density (kg/m ³)	The Bottom Layer Density (kg/m ³)	The Thickness of the Upper Layer (m)		
2005	16–17 May	Urayasu–Ichigawa–Funabashi	2.99	15.6//32.2	15.6//33.4	1023.71	1024.63	5.00	$w \geq 1.76$ m/s
2007	1–2 October	Funabashi	3.76	21.6//29	21.6//32.8	1019.80	1022.69	5.00	$w \geq 3.12$ m/s
2008	13–14 November	Funabashi–Ichigawa	3.38	18//32.2	19.2//33.00	1023.16	1023.47	5.00	$w \geq 1.02$ m/s
2011	31 May–2 June	Funabashi	3.30	-	-	1021.12	1023.06	5.00	$w \geq 2.56$ m/s
2011	21–24 October	Funabashi–Makuhari	3.76	-	-	1020.92	1022.30	3.95	$w \geq 1.70$ m/s
2012	23–25 May	Makuhari	4.37	19.2//28.2	16.8//31.8	1019.81	1023.13	5.00	$w \geq 3.35$ m/s
2013	24–27 September	Makuhari–Funabashi	4.73	-	-	1018.93	1021.53	3.41	$w \geq 2.02$ m/s
2014	27 August–3 September	Makuhari–Funabashi	-	26.4//27	22.8//31.8	1016.92	1021.59	4.00	$w \geq 3.18$ m/s
2016	14–15 June	Funabashi	3.72	-	-	1019.20	1022.75	4.50	$w \geq 3.11$ m/s

Note: Values for the stratification conditions in 2011, 2013, and 2016 are taken from Tables 1 and 2 due to a lack of real-time data measured at the CLB (<http://www4.kaiho.mlit.go.jp/kaihoweb>). Data for the wind conditions in August 2014 are not available at Edogawarinkai station, as provided by the Japanese Meteorological Agency (<http://www.data.jma.go.jp/obd/stats>).

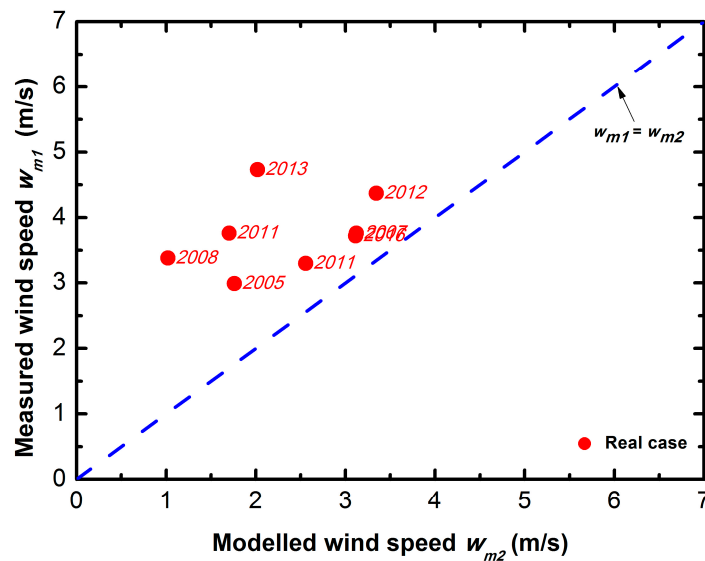


Figure 4. Comparison of measured wind speed w_{m1} and modelled wind speed w_{m2} for real cases of blue tides observed on the northeast shore of Tokyo Bay during 2003–2016, except 2014.

With regard to the real cases of blue tides on the northeast shore of Tokyo Bay during 1978–2002 that lack real-time measurement data, Table 4 presents all the information regarding the real cases using the representative stratification values for each month in Tables 1 and 2. Occurrence dates and occurrence areas of the blue tides are listed in the first column. The second column shows the calculated average wind speed of northeasterly wind, w_{m1} , before the occurrences of the blue tides. Representative values for stratification conditions of the two-layered fluid at the head of Tokyo Bay are shown in the third column, and using these values, the analytical solution for each real case, i.e., modelled wind speed, w_{m2} , could be calculated accordingly as presented in the last column. The results regarding whether real cases satisfy the calculated analytical solution can be found in Figure 5. In general, 31 of 33 real blue tide cases were in accordance with the calculated analytical solutions. Considering that there are simplifications and assumptions involved, we suggest that the proposed analytical solution shows its validity.

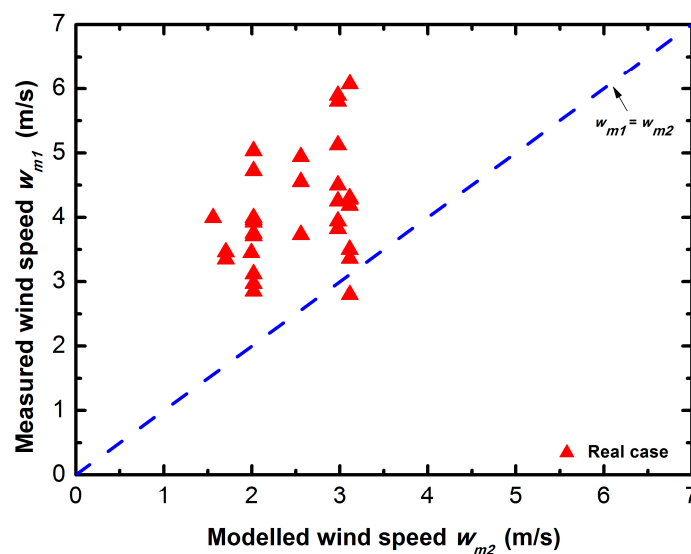


Figure 5. Comparison of measured wind speed w_{m1} and modelled wind speed w_{m2} for real cases of blue tides observed on the northeast shore of Tokyo Bay during 1978–2002, except April 2001.

Table 4. Information regarding real cases of blue tides observed on the northeast shore of Tokyo Bay during 1978–2002.

Blue Tide on the Northeast Shore During 1978–2002			Northeasterly Wind	Stratification Condition Using Representative Values			The Analytical Solution
Occurrence Date	Occurrence Area	Average Wind Speed (m/s)	The Upper Layer Density (kg/m ³)	The Bottom Layer Density (kg/m ³)	The Thickness of the Upper Layer (m)		
1978	31 May	Urayasu~Funabashi	3.73	1021.12	1023.06	5.00	$w \geq 2.56$ m/s
1978	13 June	Funabashi	3.36	1019.20	1022.75	4.50	$w \geq 3.11$ m/s
1978	16–17 July	Makuhari	4.30	1017.67	1021.96	4.09	$w \geq 3.11$ m/s
1978	14–16 August	Makuhari	4.25	1016.91	1020.91	4.05	$w \geq 2.98$ m/s
1980	2–5 August	Funabashi~Makuhari	5.80	1016.91	1020.91	4.05	$w \geq 2.98$ m/s
1980	19 September	Funabashi	3.96	1018.93	1021.53	3.41	$w \geq 2.02$ m/s
1982	21–23 May	Ichigawa	4.55	1021.12	1023.06	5.00	$w \geq 2.56$ m/s
1982	27–29 July	Ichigawa~Makuhari	3.50	1017.67	1021.96	4.09	$w \geq 3.11$ m/s
1982	6 September	Funabashi	5.03	1018.93	1021.53	3.41	$w \geq 2.02$ m/s
1984	24–26 August	Funabashi~Makuhari	3.82	1016.91	1020.91	4.05	$w \geq 2.98$ m/s
1984	9 September	Funabashi	3.12	1018.93	1021.53	3.41	$w \geq 2.02$ m/s
1985	15–18 June	Funabashi	6.07	1019.20	1022.75	4.50	$w \geq 3.11$ m/s
1986	4 August	Urayasu~Ichigawa	3.94	1016.91	1020.91	4.05	$w \geq 2.98$ m/s
1988	24 May	Funabashi	4.94	1021.12	1023.06	5.00	$w \geq 2.56$ m/s
1988	3–8 September	Funabashi	3.75	1018.93	1021.53	3.41	$w \geq 2.02$ m/s
1989	20 June	Funabashi	4.28	1019.20	1022.75	4.50	$w \geq 3.11$ m/s
1989	26–27 August	Funabashi	4.50	1016.91	1020.91	4.05	$w \geq 2.98$ m/s
1989	22–24 September	Funabashi~Makuhari	3.92	1018.93	1021.53	3.41	$w \geq 2.02$ m/s
1989	30 October	Funabashi~Makuhari	3.35	1020.92	1022.30	3.95	$w \geq 1.70$ m/s
1990	28 June–2 July	Funabashi~Makuhari	4.18	1019.20	1022.75	4.50	$w \geq 3.11$ m/s
1990	6 August	Ichigawa~Funabashi~Makuhari	5.89	1016.91	1020.91	4.05	$w \geq 2.98$ m/s
1990	7–8 September	Urayasu~Funabashi	4.72	1018.93	1021.53	3.41	$w \geq 2.02$ m/s
1990	27–29 September	Funabashi~Makuhari	3.99	1018.93	1021.53	3.41	$w \geq 2.02$ m/s
1992	1 June	Funabashi~Makuhari	2.80	1019.20	1022.75	4.50	$w \geq 3.11$ m/s
1992	2 July	Funabashi	4.18	1017.67	1021.96	4.09	$w \geq 3.11$ m/s
1992	3–6 August	Ichigawa~Funabashi	5.12	1016.91	1020.91	4.05	$w \geq 2.98$ m/s
1994	4–8 November	Makuhari~Funabashi	3.45	1021.94	1023.10	5.05	$w \geq 1.99$ m/s
1996	10–12 September	Funabashi~Makuhari	3.71	1018.93	1021.53	3.41	$w \geq 2.02$ m/s
1999	30 September	Funabashi	2.97	1018.93	1021.53	3.41	$w \geq 2.02$ m/s
1999	18–20 October	Funabashi	3.46	1020.92	1022.30	3.95	$w \geq 1.70$ m/s
2000	27–29 September	Funabashi	2.85	1018.93	1021.53	3.41	$w \geq 2.02$ m/s
2001	23–24 April	Funabashi	4.39	-	-	-	-
2001	9–10 October	Makuhari and Funabashi and Ichigawa	3.99	1021.94	1023.10	3.95	$w \geq 1.56$ m/s

As already mentioned, the computational cost of the analytical solution was to estimate densities of the upper and lower layers and the thickness of the upper, well-mixed layer based on stratification data provided by the CLB. This cost is not large, and the analytical solution is a simple and feasible method for estimating critical wind conditions under which blue tides can occur at the head of the bay.

3.3. Comparison with Real Cases Lacking Blue Tides

To further verify the validity of the proposed analytical solution, we simply compared it with real cases in which continual blowing of a northeasterly wind did not lead to occurrences of blue tides on the northeast shore of Tokyo Bay, as shown in Table 5. The first column shows the dates and average wind speed conditions, w_{m1} , for each real case, based on measurement data on wind conditions at Edogawarinkai station provided by the Japanese Meteorological Agency (<http://www.data.jma.go.jp/obd/stats>). For each real case, the second column presents the data on the stratification conditions, including the measured surface and the bottom temperature and salinity values, the calculated density values for the upper, well-mixed water layer and the bottom, oxygen-depleted water layer, and the estimated values for the thickness of the upper, well-mixed layer based on real-time measured data at the CLB as provided by the HOD, Japan (<http://www4.kaiho.mlit.go.jp/kaihoweb>). The third column shows the modelled minimum wind stresses, w_{m2} , calculated using those values for the blue tide cases occurring on the northeast shore. The results regarding whether real cases satisfy the calculated analytical solution are presented in Figure 6. For most (84.94%) of the real cases in which continual blowing of the northeasterly wind did not lead to the occurrence of blue tides, the measured wind speed is insufficient to produce coastal upwelling on the northeast shore of the bay when compared to the analytical solution. Considering that there are simplifications and assumptions involved, it could be suggested that the proposed analytical solution shows its validity also for real cases in which continual blowing of the northeasterly wind did not lead to the occurrence of blue tides. Further relaxing such simplification conditions and assumptions should be the goal of future research.

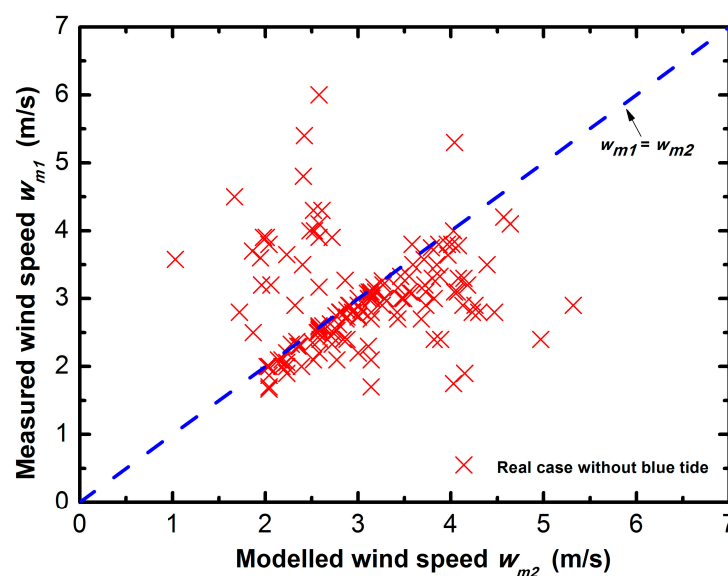


Figure 6. Comparison of measured wind speed w_{m1} and modelled wind speed w_{m2} for real cases in which continual blowing of the northeasterly wind did not lead to the occurrence of blue tides on the northeast shore of Tokyo Bay during 2003–2016.

Table 5. Information regarding real cases in which continual blowing of the northeasterly wind did not lead to the occurrence of blue tides on the northeast shore of Tokyo Bay during 2003–2016.

Real Case without Blue Tide		Stratification Condition					The Analytical Solution	
Date	Northeasterly Wind	Surface Temperature//Surface Salinity (°C)//(psu)	Bottom Temperature//Bottom Salinity (°C)//(psu)	The Upper Layer Density (kg/m ³)	The Bottom Layer Density (kg/m ³)	The Thickness of the Upper Layer (m)		
	Average Wind Speed (m/s)							
2003	May	4.00	19.2//29.8	16.8//32.2	1021.03	1023.44	7.00	$w \geq 4.03$ m/s
	June	3.16	24//29.4	20.4//32.6	1019.44	1022.86	5.00	$w \geq 3.43$ m/s
	July	2.33,3.33,3.3,3.1	22.8//29.4,22.8//29.4,22.8//27.8,22.8//29.4	21.6//31.8,20//33,20//32.6,20//33	1019.78,1019.78,1018.57,1019.78	1021.93,1023.27,1022.96,1023.27	5,5,4,5,4,5	$w \geq 2.72,3.46,3.49,3.12$ m/s
	August	3.08,3.17,3	26.4//27,22.8//27,22.8//27	24//31,21.6//32.6,20.4//32.6	1016.92,1017.96,1017.96	1020.65,1022.53,1022.86	5,4,4	$w \geq 3.58,3.17,3.28$ m/s
	September	3,2,5	26.4//26.2,20.4//30.6	22//31.8,20//32.2	1016.32,1021.33	1021.82,1022.66	4,6	$w \geq 3.47,2.57$ m/s
	October	3.90	19.2//31.4	19//32.6	1022.25	1023.22	5.50	$w \geq 2.01$ m/s
	November	4.50	19.2//31.8	19//33.4	1022.56	1023.83	4.00	$w \geq 1.67$ m/s
2004	May	3.27,2.9,2.83	16.8//30.6,19.2//31,19//30.2	16//32.2,18//32.2,16.8//33	1022.21,1021.95,1021.39	1023.62,1023.16,1024.06	6,5,5,5,5	$w \geq 2.86,2.32,3.03$ m/s
	June	3.80	21.6//27.8	18//32.6	1018.89	1023.46	5.00	$w \geq 3.96$ m/s
	July	3.50	25.2//28.2	20.4//31.4	1018.18	1021.94	5.00	$w \geq 3.59$ m/s
	September	3.1,2.8,2.7,2.5	26//29,26//29,26//30.2,23//31.8	25.2//31,25.2//31,24//32.6,22.6//33	1018.54,1018.54,1019.45,1021.54	1020.29,1020.29,1021.85,1022.56	6,5,6,5,5	$w \geq 3.19,2.94,2.87,1.87$ m/s
	October	3,2,8,2,1	20.4//29,22.6//28.6,20.4//29	21//33,22//31.4,20//31.8	1020.12,1019.23,1020.12	1023.00,1021.51,1022.35	5,5,5	$w \geq 3.15,2.80,2.77$ m/s
	November	2.45	19.2//29.8	20.4//33	1021.03	1023.16	5.00	$w \geq 2.71$ m/s
2005	May	3.07,3.8,2.63	18//30,17//29.8,16.8//31	15.6//33,15.6//33.4,15.6//33.4	1021.48,1021.56,1022.52	1024.33,1024.64,1024.64	5,5,5,5	$w \geq 3.13,3.58,2.70$ m/s
	July	3.5,3.58	24//29,24//27	19.2//33,20.4//31	1019.14,1017.63	1023.47,1021.64	5,5	$w \geq 3.85,3.71$ m/s
	September	3.20	26//25	24//29.8	1015.54	1019.74	5.50	$w \geq 4.18$ m/s
	October	2.4,4.3	22//30.6,21.6//30.2	20.4//32.6,21//31.8	1020.91,1020.71	1022.86,1022.09	5,5	$w \geq 2.59,2.61$ m/s
2006	May	5.40	15.6//31.4	14.4//32.2	1023.10	1023.97	7.00	$w \geq 2.42$ m/s
	June	3.9,3,2,9	18//31.8,19.2//30.6,22.8//28	15.6//33.4,16//33,17//33	1022.85,1021.64,1018.72	1024.64,1024.24,1024.01	4,5,5,5	$w \geq 1.98,3.29,4.26$ m/s
	July	2.4,3,1	27.6//26.2,25.2//27.8	19.2//32.6,18//33	1015.95,1017.88	1023.17,1023.17	5,4,5	$w \geq 4.97,4.04$ m/s
	September	3.33,2.8,2.9,3.3	25.2//27.4,25.2//29.8,22.8//29.8,21.6//29	20.4//32.8,21.6//32.2,21.6//32.6,20.4//33	1017.58,1019.39,1020.08,1019.80	1023.01,1022.23,1022.53,1023.16	4,5,4,5,5,6	$w \geq 3.88,2.81,2.90,4.08$ m/s
	October	2.62,2.9,4.3	22//30.2,21.6//27,21.6//29.8	20.4//32.6,20.4//31,20.4//31.8	1020.60,1018.29,1020.41	1022.86,1021.64,1022.25	5,5,5,5	$w \geq 2.79,3.73,2.52$ m/s
	November	2.00	15.6//31	18//33	1022.79	1023.77	6.50	$w \geq 2.39$ m/s
2007	July	3,3,26,2,8,5,3	24//31,22.8//30.2,24//27,25.2//27.4	19.2//33,19.2//33,19.2//33,19.2//33	1020.65,1020.38,1017.63,1017.58	1023.47,1023.47,1023.47,1023.47	5,5,5,4,5	$w \geq 3.11,3.26,4.47,4.04$ m/s
	August	3.64	27.6//27.8	21.6//33	1017.15	1022.84	4.50	$w \geq 3.97$ m/s
	September	2.9,3,5	25.2//25,25.2//25.8	24//31,21.6//30.6	1015.77,1016.38	1020.65	1021.02	$w \geq 5.32,3.59$ m/s
	October	2.53	21.6//29.8	20.4//33	1020.41	1023.16	4.50	$w \geq 2.77$ m/s
	November	2.75,4	18//31,18//30.6	19.2//32.2,19.2//32.6	1022.24,1021.93	1022.86,1023.17	6,5,6	$w \geq 2.76,2.48$ m/s

Table 5. Cont.

Real Case without Blue Tide		Stratification Condition						The Analytical Solution
Date	Northeasterly Wind	Surface Temperature/Surface Salinity (°C)/(psu)	Bottom Temperature/Bottom Salinity (°C)/(psu)	The Upper Layer Density (kg/m ³)	The Bottom Layer Density (kg/m ³)	The Thickness of the Upper Layer (m)		
	Average Wind Speed (m/s)							
2008	May	3.75,4.8,2.6,2.6,6	17//29.8,18//29.8,16.8//31,16.8//31,16.8//31	15//33,16//31,4,15//33,15//33,15//33	1021.56,1021.32,1022.52,1022.52,1022.52	1024.46,1023.01,1024.46,1024.46,1024.46	6,5,5,5,5	$w \geq 3.79,2.41,2.58,2.58,2.58$ m/s
	June	3,3,8,4.2	20.4//27,21.6//26,2,21.6//26.2	18//31.8,18//32.6,18//33	1018.60,1017.68,1017.67	1022.85,1023.46,1023.77	5,4,5,5	$w \geq 3.82,4.01,4.57$ m/s
	July	2.40	27.6//25.8	19.2//31.8	1015.65	1022.56	4.00	$w \geq 3.89$ m/s
	September	2.40	25.2//28.2	24//32.6	1018.18	1021.85	4.00	$w \geq 2.84$ m/s
	October	3.58	21.6//32.8	21//33	1022.69	1023.00	5.00	$w \geq 1.03$ m/s
2009	June	3.1,2.8	21.6//28.6,21.6//29	18//32.2,17//33	1019.50,1019.80	1023.16,1024.01	5,4,5	$w \geq 3.55,3.42$ m/s
	July	2.3,3.1	24//29.8,26.4//27	19.2//31.8,20.4//31.4	1019.74,1016.92	1022.56,1021.94	5,4,5	$w \geq 3.11,3.73$ m/s
	August	3.5,2.4	26.4//27,26.4//29	21.6//32.6,22.8//32.6	1016.92,1018.42	1022.53,1022.20	5,4	$w \geq 4.39,2.88$ m/s
	September	3.7,2.3,2.6,2.1	22.8//31.4,23//31,4,22//32.2,22.8//31	21.6//32.6,21.6//33,20.4//32.8,21.6//33	1021.29,1021.24,1022.12,1020.99	1022.53,1022.84,1023.01,1022.84	4,5,5,5,5	$w \geq 1.86,2.35,2.62,2.52$ m/s
	October	2.3,3.2	22//30,2,22//30.6	21.6//32.2,21.6//31.8	1020.60,1020.91	1022.23,1021.93	5,5,5	$w \geq 2.37,2.06$ m/s
2010	May	2.35,2.83	19.2//29.4,19.2//29.8	18//31,16.8//32.2	1020.73,1021.03	1022.24,1023.44	5,5,5	$w \geq 2.51,2.88$ m/s
	June	3.33,2.4	19.2//29.8,21.6//29	16.8//33,16.8//33	1021.03,1019.80	1024.06,1024.06	5,5,5	$w \geq 3.55,3.82$ m/s
	August	3.08	27.6//28.6	23//32.6	1017.75	1022.14	4.00	$w \geq 3.10$ m/s
	October	2.1,2,2.5,3.2	21.6//31,21.6//31,22.8//30.8,21.6//31.4	21//32.6,21//32.6,21//33,21//33	1021.32,1021.32,1020.84,1021.62	1022.70,1022.70,1023.00,1023.00	5,5,5,4,5	$w \geq 2.18,2.18,2.73,1.96$ m/s
2011	May	3.17,2.55,2.6	-	-	1021.12	1023.06	5.00	$w \geq 2.58$ m/s
	June	2.7,2.8,3,1.7	-	-	1019.20	1022.75	4.50	$w \geq 3.14$ m/s
	July	3.00	-	-	1017.67	1021.96	4.09	$w \geq 3.14$ m/s
	August	2.2,3,2.9	-	-	1016.91	1020.91	4.05	$w \geq 3.00$ m/s
	October	2.80	-	-	1020.92	1022.30	3.95	$w \geq 1.72$ m/s
	November	2.00	-	-	1021.94	1023.10	5.05	$w \geq 2.02$ m/s
2012	June	2.73,3.1,3.9	19.2//31,21.6//27,21.6//30.2	16.8//33.4,20.4//31,19.2//32.2	1021.95,1018.29,1020.71	1024.36,1021.64,1022.86	5,6,5	$w \geq 2.88,4.07,2.72$ m/s
	July	3.30	26.4//29	22.8//32.2	1018.42	1021.90	5.50	$w \geq 3.80$ m/s
	August	3.20	27.6//29	22.8//32.2	1018.05	1021.90	4.50	$w \geq 3.27$ m/s
	September	2.50	26.4//30	23//32.6	1019.17	1022.14	4.00	$w \geq 2.56$ m/s
	October	2.33,4,2,3.7	23//31.4,22.8//31,20.4//31	22//32.2,21.6//32.6,20//32	1021.23,1020.99,1021.64	1022.12,1022.53,1022.50	6,5,5,5,6,8	$w \geq 2.28,2.53,2.34$ m/s
	November	2.90	15.8//31	15//33	1022.75	1024.46	6.00	$w \geq 2.91$ m/s

Table 5. Cont.

Real Case without Blue Tide		Stratification Condition					The Analytical Solution	
Date	Northeasterly Wind	Surface Temperature//Surface Salinity (°C)//(psu)	Bottom Temperature//Bottom Salinity (°C)//(psu)	The Upper Layer Density (kg/m ³)	The Bottom Layer Density (kg/m ³)	The Thickness of the Upper Layer (m)		
	Average Wind Speed (m/s)							
2013	May	2.53,3.9	-	-	1021.12	1023.06	5.00	$w \geq 2.58$ m/s
	July	3,3.1	-	-	1017.67	1021.96	4.09	$w \geq 3.14$ m/s
	August	3.00	-	-	1016.91	1020.91	4.05	$w \geq 3.00$ m/s
	September	2.00	-	-	1018.93	1021.53	3.41	$w \geq 2.04$ m/s
	October	3.65,2.2	-	-	1020.92	1022.30	3.95	$w \geq 2.23$ m/s
2014	May	3.20	19.2//29.4	16.8//33	1020.73	1024.06	5.50	$w \geq 3.72$ m/s
	June	2.8,2.7	24//27,22.8//28	18//33.4,18//33.4	1017.63,1018.72	1024.08,1024.08	4.5,4	$w \geq 4.23,3.43$ m/s
	July	2.9,2.7	24//27,25.2//26	18//33,19.2//32	1017.63,1016.53	1023.77,1022.71	4.5,4	$w \geq 4.13,3.68$ m/s
	August	3.80	26//27	24//31	1017.04	1020.65	5.50	$w \geq 3.87$ m/s
	September	1.9,3.1	24//29,24//29	20//33,22//32	1019.13,1019.14	1023.27,1021.97	5.5,5	$w \geq 4.15,3.12$ m/s
2015	October	3.50	21.6//30	21//32	1020.56	1022.24	5.00	$w \geq 2.40$ m/s
	June	2.80	24//28	18//33	1018.38	1023.77	5.00	$w \geq 4.30$ m/s
	July	1.75	22.8//26	19.2//31	1017.21	1021.95	5.00	$w \geq 4.03$ m/s
	August	4.10	27.6//26	21.6//32	1015.80	1022.08	5.00	$w \geq 4.64$ m/s
	September	3.78,3.3	25.2//25,24//27	24//29,22.8//32	1015.78,1017.63	1019.14,1021.75	6,5,5	$w \geq 4.08,4.14$ m/s
2016	October	2.9,3.6,2.1	20.4//30.6,20.4//31.4,20.4//31.4	19.2//33,19.2//32,19.2//32	1021.33,1021.94,1021.94	1023.47,1022.71,1022.86	6,6,6	$w \geq 3.26,1.95,2.14$ m/s
	May	4.1,2.2,2.58	-	-	1021.12	1023.06	5.00	$w \geq 2.58$ m/s
	June	3.1,3.1,2.1	-	-	1019.20	1022.75	4.50	$w \geq 3.14$ m/s
	July	3,3.05	-	-	1017.67	1021.96	4.09	$w \geq 3.14$ m/s
	August	3,2.75,2.73	-	-	1016.91	1020.91	4.05	$w \geq 3.00$ m/s
2016	September	3.8,1.87,1.7,1.67	-	-	1018.93	1021.53	3.41	$w \geq 2.04$ m/s
	October	2,2.06,1.9	-	-	1020.92	1022.30	3.95	$w \geq 2.23$ m/s

Note: Real-time data on stratification conditions in 2011, 2013 and 2016 provided by the CLB were unavailable (<http://www4.kaiho.mlit.go.jp/kaihoweb>), and we used the values for the densities of the upper and bottom layers and thickness of the upper layer shown in Tables 1 and 2 for 2011, 2013 and 2016.

4. Discussion and Concluding Remarks

4.1. Discussion

Occurrences of blue tides result in substantial economic losses to coastal fisheries at the head of Tokyo Bay. Thus, it is important to estimate critical wind conditions under which coastal upwelling associated with blue tide could occur in Tokyo Bay. Compared to a mesh-based numerical modelling approach, the analytical solution adopted in this study can roughly estimate the critical wind conditions with lesser computational cost, and it also facilitates a qualitative understanding of the factors that influence the occurrence of blue tide and what these effects are. Once the densities of the upper and lower layers, the thickness of the upper, well-mixed layer and the observed wind conditions are estimated based on real-time stratification data provided by the CLB and meteorological data provided by JMA, the analytical solution can provide a simple evaluation of whether the blue tide could occur at the head of Tokyo Bay.

The weakness of the proposed analytical model is that it has been derived based on some simplifications and assumptions. These simplification and assumption conditions that are applicable to Tokyo Bay mainly include that (1) the irregularities of the bay coastline were neglected; (2) the bay water depth was assumed to be same everywhere; and (3) a simple wind-driven two-layered fluid model was assumed to be representative of the actual stratified condition of the bay. For similar engineering conditions such as reservoirs, lakes and estuarine embayments in other parts of the world, if these simplifications and assumptions are still applicable, the analytical solution proposed in this study could still show its validity for estimating critical wind conditions under which wind-driven upwelling could happen. Climate change has non-negligible effects on the surface wind field at the top of Tokyo Bay and stratification conditions of water bodies within the bay through fresh water and seawater interaction, but if the real-time wind and stratification conditions of the water body in the bay are known, the analytical solution could still provide simple criteria to predict if a blue tide could occur at the head of Tokyo Bay.

4.2. Concluding Remarks

Blue tides at the head of Tokyo Bay are a hydro-environmental phenomenon where seawater appears to be milky blue due to the reflection of sunlight off of surface water that contains large amounts of sulphur particles. Its appearance is due to the coastal upwelling of bottom oxygen-depleted water induced by northeasterly wind-driven circulation. The occurrences of blue tides cause the death of many shellfish and other aquatic animals across the head of Tokyo Bay, consequently resulting in substantial economic losses to coastal fisheries.

This paper examined the occurrence of wind-driven blue tide in Tokyo Bay, based on a simplified hydrodynamic model and observational analysis. The model assumed a two-layered fluid structure with a wind-driven upper water layer and a bottom oxygen-depleted water layer. In this study, we derived a simple analytical solution to determine the critical wind condition for which the lower layer outcrops if the wind forcing is sufficiently strong, resulting in mixing of the two layers and giving rise to blue tide. The results of sensitivity analyses of the analytical solution to all incorporated factors were found to be in accordance with qualitative understandings of the blue tide phenomenon. Moreover, the proposed analytical solution showed its validity by comparison with observational data from real cases of blue tide during 1978–2016 and without blue tide during 2003–2016. This study would be helpful for a better understanding of the hydro-dynamic mechanism of blue tide in the blue tide community. It should also be noted that although the analytical solution could present a simple relation for characterizing the dependence of wind conditions on the stratification properties and geometrical properties of the two-layered fluid, there are some large simplifications and assumptions in deriving it. Further relaxing such simplifications and assumptions should be the goal of further investigation in future research. In this regard, a more realistic three-dimensional hydrodynamic model could show its capacity to more systematically investigate the underlying dynamics of upwelling and mixing.

Acknowledgments: This work was supported by the National Natural Science Foundation of China (Number: 51509004). Considering that some of the references cited in this paper are in Japanese, interested readers should feel free to contact the authors for the English translated edition of those references.

Author Contributions: Zhongfan Zhu developed the model, analysed the results and wrote the paper. Xiaomei Bai, Jie Dou and Pengfei Hei contributed to revisions of the paper.

Conflicts of Interest: The authors declare no conflict of interest.

References

1. Yunus, A.P.; Dou, J.; Sravanthi, N. Remote sensing of chlorophyll-a as a measure of red tide in Tokyo Bay using hotspot analysis. *Remote Sens. Appl. Soc. Environ.* **2015**, *2*, 11–25. [[CrossRef](#)]
2. Koibuchi, Y.; Isobe, M. Phytoplankton Bloom Mechanism in an Area Affected by Eutrophication: Tokyo Bay. *Coast. Eng. J.* **2007**, *49*, 461–479. [[CrossRef](#)]
3. Higa, H.; Koibuchi, Y.; Kobayashi, H.; Toratani, M.; Sakuno, Y. Numerical Simulation and Remote Sensing for the Analysis of Blue Tide Distribution in Tokyo Bay in September 2012. *J. Adv. Simul. Sci. Eng.* **2015**, *2*, 1–15. [[CrossRef](#)]
4. Sasaki, J. Coastal upwelling of water body at the head of Tokyo Bay and its influence to “Aoshio”. *Proc. Coast. Eng. JSCE* **1997**, *44*, 1101–1105. (In Japanese)
5. Otsubo, K.; Harashima, A.; Miyazaki, T.; Yasuoka, Y.; Muraoka, K. Field survey and hydraulic study of “Aoshio” in Tokyo Bay. *Mar. Pollut. Bull.* **1991**, *23*, 51–55. [[CrossRef](#)]
6. Kakino, J.; Matsuyama, S.; Sato, Y.; Kase, N. Relationship between Aoshio, blue-green turbid water and wind-driven current. *Nippon Suisan Gakkaishi* **1987**, *53*, 1475–1481. (In Japanese) [[CrossRef](#)]
7. Kataoka, S.; Hirotsuka, H.; Komatsu, A. On the occurrence condition of blue tide in the inner Tokyo Bay. *Proc. Ocean Dev. JSCE* **1989**, *5*, 233–238. (In Japanese)
8. Zhu, Z. Minimum wind stress for the occurrence of blue tide on the southeast shore of Tokyo Bay. *J. Geosci. Environ. Prot.* **2014**, *2*, 126–134. [[CrossRef](#)]
9. Zhu, Z.; Yu, J. Estimating the occurrence of wind-driven coastal upwelling associated with “aoshio” on the northeast shore of Tokyo Bay, Japan: An analytical model. *Sci. World J.* **2014**, *2014*. [[CrossRef](#)] [[PubMed](#)]
10. Sasaki, J.; Isobe, M.; Watanabe, A.; Gomyo, M. The phenomenon regarding the anoxic water and a model of seasonal variations of temperature and DO in Tokyo Bay. *Proc. Coast. Eng. JSCE* **1993**, *40*, 1051–1055. (In Japanese)
11. Sasaki, J.; Isobe, M.; Watanabe, A.; Gomyo, M. Study on scale of blue tide in Tokyo Bay. *Proc. Coast. Eng. JSCE* **1996**, *43*, 1111–1115. (In Japanese)
12. Sasaki, J.; Isobe, M.; Huzimoto, H. Development of simple methods of predicting blue tide in Tokyo Bay. *Proc. Coast. Eng. JSCE* **1999**, *46*, 1006–1010. (In Japanese)
13. Sasaki, J.; Koide, M.; Nagata, M.; Shibayama, T.; Isobe, M. Numerical study on improvement effect of blue tide water using microbubbles generator in Sanbanze of Tokyo Bay. *Proc. Coast. Eng. JSCE* **2003**, *50*, 981–985. (In Japanese)
14. Takahashi, T.; Nakata, H.; Hirano, K.; Matsuoka, K.; Iwataki, M.; Yamaguchi, H.; Kasuya, T. Upwelling of oxygen-depleted water (Sumishio) in Omura Bay, Japan. *J. Oceanogr.* **2009**, *65*, 113–120. [[CrossRef](#)]
15. Matsuyama, M.; Touma, K.; Ohwaki, A. Numerical experiments of upwelling in Tokyo Bay in relation to “Aoshio” (the upwelled anoxic blue-green turbid water). *Bull. Coast. Oceanogr.* **1990**, *28*, 63–74. (In Japanese and English Abstract)
16. Nakatsuji, K.; Nagasaka, S.; Muraoka, K. Basic experiments on upwelling of anoxic water observed in Tokyo Bay, Japan. *Proc. Hydraul. Eng. JSCE* **1991**, *35*, 603–608. (In Japanese) [[CrossRef](#)]
17. Yoon, J.S.; Nakatsuji, K.; Muraoka, K. Experimental study on wind-driven stratified flow in enclosed water body. *Proc. Hydraul. Eng. JSCE* **1993**, *37*, 285–292. (In Japanese) [[CrossRef](#)]
18. Yoon, J.S.; Nakatsuji, K.; Muraoka, K. Experimental study on wind-driven stratified flow in open water body. *Proc. Coast. Eng. JSCE* **1993**, *40*, 241–245. (In Japanese)
19. Yoon, J.S.; Nakatsuji, K.; Muraoka, K. Density interface movement and mixing in a two-layered stratified flow system. *Proc. Hydraul. Eng. JSCE* **1995**, *39*, 811–818. (In Japanese) [[CrossRef](#)]
20. Nakatsuji, K.; Yoon, J.S.; Yuasa, T.; Muraoka, K. The relationship between wind-driven stratified flow and occurrence mechanism of blue tide. *Proc. Coast. Eng. JSCE* **1995**, *42*, 1066–1070. (In Japanese)

21. Tsukada, M.; Mimura, N.; Suzuki, M. Numerical simulation on formation, maintenance and attenuation of anoxic water body in Tokyo Bay. *Proc. Coast. Eng. JSCE* **1997**, *44*, 1086–1090. (In Japanese)
22. Watanabe, M.; Amano, K.; Ishikawa, Y.; Kohata, K. Analysis of autumn upwelling of anoxic bottom water, distribution and vertical circulation induced by wind in Tokyo Bay. *J. Jpn. Soc. Civ. Eng.* **1998**, *608*, 13–29. (In Japanese)
23. Koibuchi, Y.; Isobe, M. Study on “Aoshio” around Yokohama harbor at the western side of Tokyo Bay in 2004. *Proc. Coast. Eng. JSCE* **2005**, *52*, 896–900. (In Japanese)
24. Sasaki, J.; Kawamoto, S.; Yoshimoto, Y.; Ishii, M.; Kakino, J. Evaluation of the effect of anoxic water in dredged trenches on blue tides in Tokyo Bay. *Proc. Coast. Eng. JSCE* **2007**, *54*, 1041–1045. (In Japanese) [[CrossRef](#)]
25. Ichioka, S.; Sasaki, J.; Yoshimoto, Y.; Shimosako, K.; Kimura, S. Analysis of Sulfide Dynamics Including Outbreak of Blue Tide in Navigation Channels and Dredged Trench of Tokyo Bay. *J. Jpn. Soc. Civ. Eng. Ser. B2 Coast. Eng.* **2009**, *65*, 1041–1045. [[CrossRef](#)]
26. Suzuki, T.; Matsuyama, M. Numerical Experiments on Stratified Wind-induced Circulation in Tokyo Bay, Japan. *Estuar. Coast. Shelf Sci.* **2000**, *50*, 17–25. [[CrossRef](#)]
27. Sasaki, J.; Kawamoto, S.; Yoshimoto, Y.; Ishii, M.; Kakino, J. Evaluation of the Amount of Hydrogen Sulfide in a Dredged Trench of Tokyo Bay. *J. Coast. Res.* **2009**, *1*, 890–894.
28. Ueno, S.; Nadaoka, K.; Ishimura, A.; Katsui, H. Analysis on the upwelling due to wind in Tokyo Bay based on NOAA-AVHRR data. *Proc. Coast. Eng. JSCE* **1992**, *39*, 256–260. (In Japanese)
29. Csanady, G.T. *Circulation in the Coastal Ocean*; D. Reidel Publishing Company: Dordrecht, The Netherlands, 1982; pp. 25–63, ISBN 978-90-481-8372-2.
30. Mccutcheon, S.C.; Martin, J.L.; Barnwell, T.O. Water quality. In *Handbook of Hydrology*, 1st ed.; Maidment, D.R., Ed.; McGraw-Hill: New York, NY, USA, 1993; pp. 191–197, ISBN 9780070397323.
31. Angeli, C.; Leonardi, E.; Maciocco, L. A computational study of salt diffusion and heat extraction in solar pond plants. *Sol. Energy* **2006**, *80*, 1498–1508. [[CrossRef](#)]
32. Mogollón, J.M.; Dale, A.W.; Jensen, J.B.; Schlüter, M.; Regnier, P. A method for the calculation of anaerobic oxidation of methane rates across regional scales: An example from the Belt Seas and The Sound (North Sea-Baltic Sea transition). *Geo-Mar. Lett.* **2013**, *33*, 299–310. [[CrossRef](#)]
33. Stamou, A.I.; Nikiforakis, I.K. Integrated modelling of single port, steady-state thermal discharges in unstratified coastal waters. *Environ. Fluid Mech.* **2013**, *13*, 309–336. [[CrossRef](#)]
34. Conroy, J.L.; Thompson, D.M.; Collins, A.; Overpeck, J.T.; Bush, M.B.; Cole, J.E. Climate influences on water and sediment properties of Genovesa Crater Lake, Galápagos. *J. Paleolimnol.* **2014**, *52*, 331–347. [[CrossRef](#)]
35. Oh, S.H.; Kim, B.M.; Kang, N. Evaluation of changes in cylinder volume due to gas filling and subsequent release. *Metrologia* **2013**, *50*, 318–324. [[CrossRef](#)]
36. Diamantopoulos, S.; Milickovic, N.; Butt, S.; Katsilieri, Z.; Kefala, V.; Zogal, P.; Sakas, G.; Baltas, D. Effect of using different U/S probe Standoff materials in image geometry for interventional procedures: The example of prostate. *J. Contemp. Brachytherapy* **2011**, *3*, 209–219. [[CrossRef](#)] [[PubMed](#)]

